特集

Enhancement of Piezoelectric Response in Scandium Aluminum Nitride Alloy Thin Films prepared by Dual Reactive Co-Sputtering*

加納一彦 Kazuhiko KANO　秋山守人 Morito AKIYAMA　蒲原敏浩 Toshihiro KAMOHARA　勅使河原明彦 Akihiko TESHIGAHARA
竹内幸裕 Yukihiro TAKEUCHI　川原伸章 Nobuaki KAWAHARA

A high temperature piezoelectric material exhibiting a good balance between high maximum use temperature and large piezoelectricity. We achieved this through the combination of the discovery of a phase transition in scandium aluminum nitride ($Sc_xAl_{l-x}N$) alloy thin films, and the use of dual co-sputtering leading to nonequilibrium alloy thin films. $Sc_{0.43}Al_{0.57}N$ alloys exhibit a large piezoelectric coefficient d_{33} of 27.6 pCN^{-1}, which is at least 500% lager than AlN.

Key words：Scandium aluminum nitride, Piezoelectric response, Alloy, Thin films, Dual co-sputtering

The industrial demand of higher temperature piezoelectric sensors is drastically increasing in controlling automobile, aircraft and turbine engines, and monitoring of furnace and reactor systems [1], because environmental problems, such as carbon-dioxide (CO_2) and nitrogen oxide (NOx) reduction, is becoming more serious globally. Also the sensors are desirable in health monitoring coal-fired electric generation plants and nuclear plants [2]. It is generally known that piezoelectric materials with higher Curie temperature possess lower piezoelectric coefficient [3)4)5)]. Furthermore, the study result (**Fig. 1**) of relationship between maximum use temperature and piezoelectric coefficient d_{33} shows that the piezoelectric materials with higher maximum use temperature possess lower piezoelectric coefficient d_{33} [3)-9)]. For example, the Curie temperature and piezoelectric coefficient d_{33} of lead zirconium titanate (PZT), which is widely used in many electronic devices, are 250°C and 410 pCN^{-1}, respectively [10)]. The maximum use temperature and d_{33} of aluminum nitride (AlN), which is one of typical high temperature piezoelectric materials, are 1150°C and 5.5 pCN^{-1} [4)]. It is difficult to achieve a good balance between high maximum use temperature and large piezoelectricity in a material. There has been a effort in order to develop high temperature piezoelectric materials with high piezoelectricity However, no effective piezoelectric materials has yet been found [6)11)]. In this communication, we report a high temperature piezoelectric material exhibiting a good balance between high maximum use temperature and large piezoelectricity. We achieved this through the combination of the discovery of a phase transition in scandium aluminum nitride ($Sc_xAl_{l-x}N$) alloy thin films, and the use of dual co-sputtering leading to nonequilibrium alloy thin films. $Sc_{0.43}Al_{0.57}N$ alloys exhibit a large piezoelectric coefficient d_{33} of 27.6 pCN^{-1}, which is

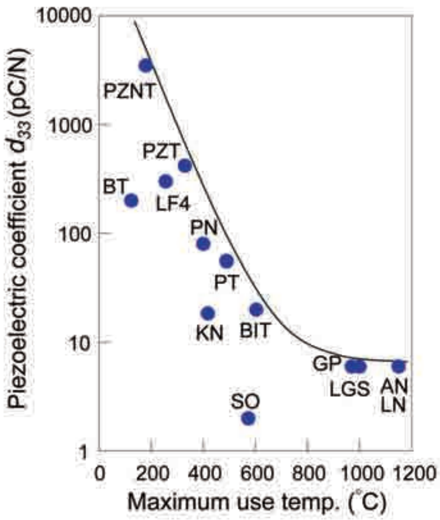

Fig. 1　Relationship between piezoelectric coefficient d_{33} and maximum use temperature for piezoelectric ceramics. Most are the Curie temperature. AlN and LGS are known maximum use temperature. AN: AlN. BT: $BaTiO_3$. BIT: $Bi_4Ti_3O_{12}$. GP: $GaPO_4$. KN: $KNbO_3$. LF4: $(K_{0.44}Na_{0.52}Li_{0.04})(Nb_{0.86}Ta_{0.10}Sb_{0.04})_3$. LGS: $La_3Ga_5SiO_{14}$. LN: $LiNbO_3$. PN: $PbNb_2O_6$. PT: $PbTiO_3$. PZNT: $0.92Pb(Zn_{1/3}Nd_{2/3})O_3$-$0.08PbTiO_3$. PZT: $Pb(Zr_{0.52}Ti_{0.52})O_3$. SO: SiO_2.

＊Copyright Clearance Center の許可を得て，Advanced Materialsより一部加筆して転載

at least 500% lager than AlN. The large piezoelectric coefficient d_{33} is the highest piezoelectric response among the tetrahedrally bonded semiconductors, despite the fact that the crystal structure of scandium nitride (ScN) is rocksalt (non-polar)[12]. Moreover, the large piezoelectricity is not changed by an annealing of 500ºC for 56 h in vacuum. This work demonstrates a new route to design a high temperature piezoelectric material.

ScN is rocksalt structure (non-polar)[12]. However, Takeuchi reported the existence of a (meta) stable wurtzite structure in ScN and the possible fabrication of Sc-IIIA-N nitrides by first-principles calculations [12]. Farrer *et al*. predicted that the wurtzite structure is unstable in ScN, and the hexagonal structure is (meta) stable in ScN, unlike the wurtzite structure [13]. The piezoelectric responses of hexagonal $Sc_xGa_{1-x}N$ and $Sc_xIn_{1-x}N$ alloys can be enhanced by an isostructural phase transition (from wurtzite to layered hexagonal) by first-principles calculations [13)14)15]. However, the piezoelectric responses and Curie temperature of the nitride alloys have not yet been confirmed by experiments [16)17]. AlN, GaN and InN are IIIA nitrides and are wurtzite structure (polar) [12]. Especially, the thermal stability and piezoelectricity of AlN are the highest among the IIIA nitrides [4]. AlN is a piezoelectric material compatible with the CMOS manufacturing process, and is a promising material for integrated sensors / actuators on silicon substrates [18]. Wurtzite and rocksalt structures have rather different lattice forms and units sizes from each other. The formation of $Sc_xAl_{1-x}N$ alloys causes a lattice distortion for the structural phase transition. Furthermore, the formation of $Sc_xAl_{1-x}N$ alloys exploit the

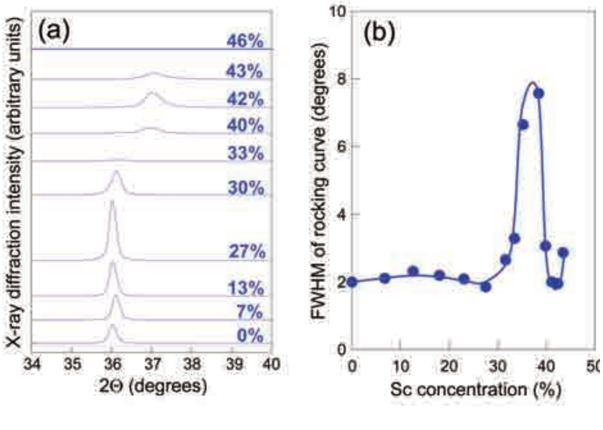

Fig. 2　a) XRD patterns of $Sc_xAl_{1-x}N$ alloys at various Sc concentrations. b) FWHM of x-ray rocking curves of $Sc_xAl_{1-x}N$ alloys at various Sc concentrations.

hybridization of electrovalent onto covalent bonding for further improvement in piezoelectricity, because the lower electronegativity of Sc compared to Al is expected to make the alloys more electrovalent [10]. Thus, we expected that an enhancement of piezoelectric responses should occur in disordered hexagonal $Sc_xAl_{1-x}N$ alloys with high maximum use temperature when increasing x composition for the development of new high temperature piezoelectric materials.

We selected dual co-sputtering method, which can grow nonequilibrium alloy thin films at a low substrate temperature, in order to prepare $Sc_xAl_{1-x}N$ alloy thin films, because $Sc_xAl_{1-x}N$ phase is not indicated in the ternary Sc-Al-N phase diagram [19], and $Sc_xAl_{1-x}N$ might be a nonequilibrium alloy. The crystal structure and orientation of $Sc_xAl_{1-x}N$ alloys were investigated by x-ray diffraction (XRD). The XRD peak intensity increases with increasing Sc concentration, indicating a maximum value at a Sc concentration of 27% (**Fig. 2a**). These indicate that the crystal structures are wurtzite and that the alloys exhibit a c-axis crystal orientation. The peak intensity drastically decreases, when the Sc concentration is between 30% and 40%. However, between 40% and 45%, the peak intensity increases around 37º again. It is generally thought that the piezoelectric response of AlN films strongly depends on crystal orientation, which is evaluated by the full width at half maximum (FWHM) of the x-ray rocking curve of (0002) AlN reflection [20]. The crystal orientation is not high compared to that of single crystal AlN films [21], and independent on the Sc concentration (**Fig. 2b**). The FWHM values drastically increase at Sc concentration between 30% and 40%, suggesting that the crystal orientation of the $Sc_xAl_{1-x}N$ alloys becomes lower between 30% and 40%.

Fig. 3 shows the dependence of the piezoelectric coefficient d_{33} of $Sc_xAl_{1-x}N$ alloys on Sc concentration. The d_{33} gradually increases with increasing Sc concentration from 0% to 43%. When the Sc concentration is 43%, the alloys exhibit a peak d_{33} of 24.6 pCN^{-1}, which is the highest reported to date for nitride semiconductors. Zinc oxide (ZnO), which is used in cell phones as filter materials, has the strongest piezoelectric response of 12.4 pCN^{-1} among the tetrahedrally bonded semiconductors [22)23]. Thus, the d_{33} of $Sc_{0.43}Al_{0.57}N$ alloys is the strongest piezoelectric response among the tetrahedrally bonded semiconductors. We investigated the influence of substrate temperature and annealing on the piezoelectricity of $Sc_{0.43}Al_{0.57}N$ alloys, because the alloys might be a nonequilibrium material [19]. The piezoelectricity is hardly influenced by substrate temperature (**Fig. 4a**), and exhibits a maximum value of 27.6 pCN^{-1} at 400℃. The piezoelectricity is not changed by an annealing of 500℃ for 56 h in vacuum (**Fig. 4b**), and hence $Sc_{0.43}Al_{0.57}N$ alloys is

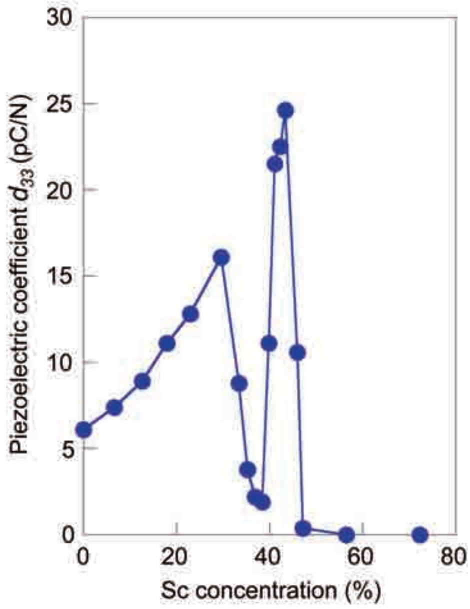

Fig. 3 Dependence of piezoelectric coefficient d_{33} of $Sc_xAl_{1-x}N$ alloys on Sc concentration.

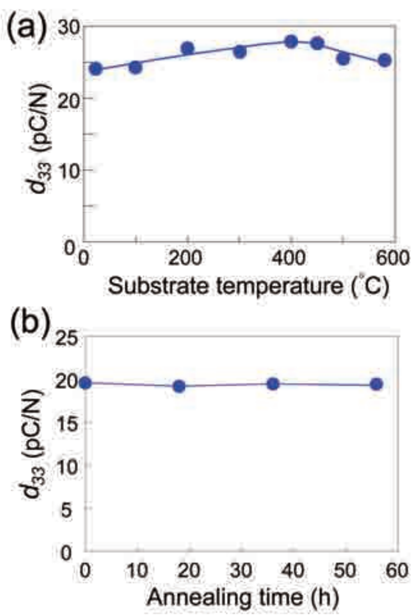

Fig. 4 a) Dependence of piezoelectric coefficient d_{33} of $Sc_{0.43}Al_{0.57}N$ alloys on substrate temperature. b) Influence of annealing of 500° C for 56 h in vacuum on piezoelectric coefficient d_{33} of $Sc_{0.40}Al_{0.50}N$ alloys prepared at 580° C.

thermally stable.

The microstructures of $Sc_xAl_{l-x}N$ alloys were observed by transmission electron microscopy (TEM). The a and c axis length is calculated by using the images of electron beam diffractions. According to electron beam diffraction images, the crystal structures are only hexagonal phase below 41% (**Fig. 5a**, **Fig. 5e**). On the other hand, above 46%, the crystal structures change to cubic phase. Between 42% and 45%, both of hexagonal and cubic phases coexist (**Fig. 5b-5h**). Interestingly, the hexagonal phases grow on the cubic phases. The a-axis gradually grows longer, c-axis becomes shorter and the c/a axis ratio decreases with increasing Sc concentration (**Fig. 6**). The c/a axis ratio is 1.4 at a Sc concentration of 43%. When the c/a axial ratio of hexagonal ScN is 1.4, the d_{33} of hexagonal ScN is 22.2 pCN^{-1}, which is close to the d_{33} (24.6-27.6 pCN^{-1}) of $Sc_{0.43}Al_{0.57}N$ alloys [24]. These results support the effect of strained hexagonal ScN. Furthermore, Constantin *et al*. reported that the state of $Sc_xGa_{l-x}N$ alloys is (i) wurtzite-like for Sc compositions smaller than 17%, (ii) cubic, rocksalt-like for Sc concentrations larger than 54%, and (iii) a transitional regime between 17% and 54% [17]. This paper supports that there is transitional regime between wurtzite and rocksalt structures. The c/a axis ratio of wurtzite AlN and hexagonal ScN is 1.60 and 1.21, respectively [13]. Since the c/a axis ratio of $Sc_xAl_{l-x}N$ alloys is between 1.60 and 1.33 (**Fig. 6**), we think that the crystal structure of $Sc_xAl_{l-x}N$ alloys is a hexagonal intermediate phase between wurtzite AlN (polar) and rocksalt ScN (non-polar), and that the intermediate phase induce the large piezoelectric response [13)14)15)].

In conclusion, $Sc_xAl_{l-x}N$ alloy thin films exhibit large piezoelectric responses. The alloys are prepared by dual co-sputtering. When the Sc concentration is 43%, the alloys exhibit a peak d_{33} of 24.6 pCN^{-1}, which is the highest reported to date for nitride semiconductors. Moreover, the alloys exhibit a good balance between high maximum use temperature and large piezoelectricity. The large piezoelectricity is not changed by an annealing of 500℃ for 56 h in vacuum. The large piezoelectric responses will open the way for a broad class of applications including use in high temperature piezoelectric devices.

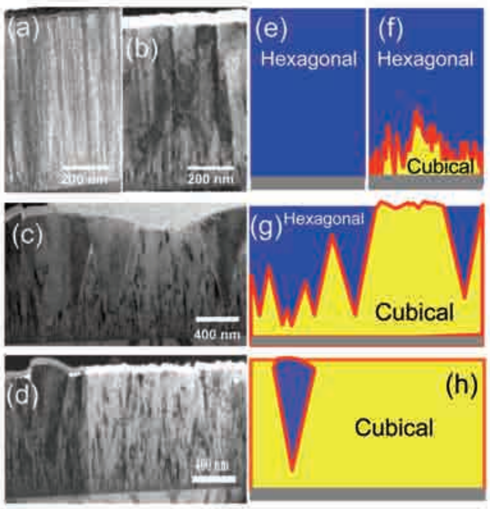

Fig. 5　Influence of Sc concentration on crystal growth of $Sc_xAl_{1-x}N$ alloys. a)-d) Cross-sectional TEM images of $Sc_xAl_{1-x}N$ alloys. e)-h) Diagrams of state of hexagonal and cubic phases of TEM images. (The blue and yellow represent wurtzite and cubic phases, respectively.) (a),(e) at a Sc concentration of 41%, (b),(f) 42%, (c),(g) 43%, (d),(h) 45%.

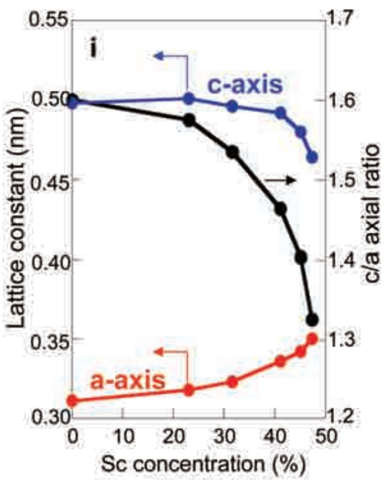

Fig. 6　Dependence of lattice constants of $Sc_xAl_{1-x}N$ alloys on Sc concentration. (The blue, red and black represent c-axis length, a-axis length, c/a axial ratio, respectively.) The a and c axis length is calculated by using the images of electron beam diffractions.

Experimental

$Sc_xAl_{1-x}N$ alloy thin films (0.5-1.1 μm in thickness) were prepared on n-type (100) silicon substrates by dual radio frequency magnetron reactive co-sputtering at 580°C in 40% N_2 at a growth pressure of 0.25 Pa. The Sc concentration in the alloy films was controlled by the Al and Sc target powers (0-200 W). The optimized sputtering conditions of AlN films were reported in our previous studies [25]. The aluminum and scandium sputtering targets were 50.8 mm in diameter. The sputtering chamber was evacuated to a pressure below 1.2×10^{-6} Pa, and then high-purity argon (99.999%) and nitrogen (99.999%) were introduced. Before deposition, the targets were cleaned under the same deposition conditions for 3 min with the shutter closed.

Characterization: For the piezoelectric coefficient d_{33} measurement, evaporated Cu top electrodes (6 mm in diameter) were used, and the piezoelectric coefficient d_{33} was measured with a piezometer system. The crystal structure and orientation of the AlN films were investigated by x-ray diffraction (XRD) with CuKα radiation. The microstructures were observed by transmission electron microscopy (TEM), and TEM samples were prepared with a focused ion beam mill. The scandium concentration in the alloy films was analyzed by energy dispersive x-ray fluorescence spectrometer (EDX). The a and c axis length is calculated by using the images of electron beam diffractions. The Young's modulus of alloy films is measured with a nano-indentation, and the modulus was 225 GPa.

REFERENCES

1) R.Mock, H. Meixner, *Sens. Actuat. A* **1991**, 25-27, 103.
2) M. J. Schulz, M. J. Sundaresan, J. Mcmichael, D. Clayton, R. Sadler, B. Nagel, *J. Intell. Mater. Syst. Struct.* **2003**, *14*, 693.
3) S. Zhang, R. Xia, L. Lebrun, D. Anderson, T. R. Shrout, *Mater. Lett.* **2005**, *59*, 3471.
4) R. C. Turner, R. E. Fuierer, R. E., Newnham, T. R. Shrout, *Appl. Acoust.* **1994**, *41*, 299.
5) S. Wada, *Bull. Ceram. Soc. Jpn.* **2008**, *43*, 639.
6) S. Zhang, Y. Fei, B. H. T. Chai, E. Frantz, D. W. Snyder, X. Jiang, T. R. Shrout, *Appl. Phys. Lett.* **2008**, *92*, 202905.
7) R. C. Turner, P. A. Fuierer, R. E. Newnham, T. R. Shrout, *Apple. Acoust.* **1994**, *41*, 299.
8) S. Zhang, L. Lebrun, C. A. Randall, T. R. Shrout, *J. Crystal Growth* **2004**, *267*, 204.
9) E. Ansorge, S. Schimpf, S. Hirsch, J. Sauerwald, H. Fritze, B. Schmit, *Sens. Actuators. A* **2006**, *130-131*, 393.

10）Y. Saito, H. Takao, T. Tani, T. Nonoyama, K. Takatori, T. Homma, T. Nagaya, M. Nakamura, *Nature* **2004**, *432*, 84.

11）I. H. Jung, W. J. Yang, A. Yoshikawa, T. Fukuda, K. H. Auh, *J. Crystal Growth* **2004**, *262*, 40.

12）N. Takeuchi, *Phys. Rev. B* **2002**, *65*, 045204.

13）N. Farrer, L. Bellaiche, *Phys. Rev. B* **2002**, *66*, 201203.

14）V. Ranjan, S. Bin-Omran, D. Sichuga, R. S. Nichols, L. Bellaiche, *Phys. Rev. B* **2005**, *72*, 085315.

15）A. Alsaad, A. Ahmad, *Eur. Phys. J. B* **2006**, *54*, 151.

16）M. E. Little, M. E. Kordesch, *Appl. Phys. Lett.* **2001**, *78*, 2891.

17）C. Constantin, H. Al-Brithen, M. B. Haider, D. Ingram, A. R. Smith, *Phys. Rev. B* **2004**, *70*, 193309.

18）M. Sternitzke, G. Muller, *J. Am. Cerm. Soc.* **1994**, *77*, 737.

19）J. C. Schuster, J. Bauer, *J. Less-Common Met.* **1985**, *109*, 345.

20）F. Martin, P. Muralt, M. A. Dubois, A. Pezous, *J. Vac. Sci. Technol. A* **2004**, *22*, 361.

21）H. Okano, Y. Takahashi, T. Tanaka, K. Shibata, S. Nakano, *Jpn. J. Appl. Phys.* **1992**, *31*, 3446.

22）K. Jeganathan, T. Kitamura, M. Shimizu, H. Okumura, *Jpn. J. Appl. Phys.* **2002**, *41*, L28.

23）A. D. Corso, M. Posternak, R. Resta, A. Baldereschi, *Phys. Rev. B* **1994**, *50*, 10715.

24）V. Ranjan, L. Bellaiche, E. J. Walter, *Phys. Rev. Lett.* **2003**, *90*, 257602.

25）M. Akiyama, T. Harada, C. N. Xu, K. Nonaka, T. Watanabe, *Thin Solid Films* **1999**, *350*, 85.

<著　者>

加納　一彦
(かのう　かずひこ)
エレクトロニクス研究部
電気学会，セラミックス協会会員
MEMS技術を用いた自動車用センサ・アクチュエータの研究開発に従事

勅使河原　明彦
(てしがはら　あきひこ)
エレクトロニクス研究部
応用物理学会会員
MEMS技術，圧電薄膜技術を用いた自動車用センサの研究開発に従事

竹内　幸裕
(たけうち　ゆきひろ)
エレクトロニクス研究部
応用物理学会，自動車技術会各会員
化合物半導体のデバイス·結晶成長，Si半導体センサの研究開発に従事

秋山　守人
(あきやま　もりと)
九州工業技術試験所（現，産業技術総合研究所）に入所
工学博士
機能性セラミックス薄膜および蛍光体の研究開発に従事

蒲原　敏浩
(かもはら　としひろ)
産業技術総合研究所
テクニカルスタッフ
機能性セラミック薄膜の研究開発に従事

川原　伸章
(かわはら　のぶあき)
情報通信機器開発部
工学博士
マイクロデバイス，マイクロマシンの研究開発に従事